Functionalized Au^{MBA}@Ag Nanoparticles as an Optical and SERS Dual Probe in a Lateral Flow Strip for the Quantitative Detection of *Escherichia coli* O157:H7

Hai-bin Liu, Chun-yang Chen, Chen-ning Zhang, Xin-jun Du, Ping Li, and Shuo Wang

Abstract: A method combining surface-enhanced Raman scattering (SERS) with a lateral flow strip (LFS) was developed for the quantitative and sensitive analysis of *Escherichia coli* O157:H7. Au^{MBA}@Ag nanoparticles were prepared as SERS probes, and 4-methylthiobenzoic acid (MBA) as a Raman reporter was inserted into the interior gap of the Au@Ag core-shell nanoparticles, which replaced the Au nanoparticles that serve as SERS nanotags in traditional LFS. Using this developed SERS-LFS, the presence of the target bacteria could be tested through the appearance of a red band on the test line. Furthermore, quantitative analysis of *E. coli* O157:H7 was achieved by measuring the specific Raman intensity of MBA on the test line. The sensitivity of this SERS-LFS biosensor is 5×10^4 CFU/mL of *E. coli* O157:H7, which is 10-fold higher than that of a naked eye-based colorimetric LFS. This quantitative detection of *E. coli* O157:H7 ($\mathcal{Y} = 1993.86\mathcal{X} - 6812.17$, $R^2 = 0.9947$) was obtained with a wide linear range (5×10^4 to 5×10^8) due to the signal enhancement of the SERS nanotags. In addition, the SERS-LFS could differentiate *E. coli* O157:H7 from closely related bacterial species or nontarget contaminants, suggesting high specificity of this assay. The applicability of SERS-LFS to the analysis of *E. coli* O157:H7 in milk, chicken breast, and beef was also validated, indicating that the sensitivity was not disturbed by the food matrix. In summary, the SERS-LFS developed in this study could be a powerful tool for the quantitative and sensitive screening of *E. coli* O157:H7 in a food matrix.

Keywords: *Escherichia coli* O157:H7, lateral flow strip, quantitative and sensitive detection, surface-enhanced Raman scattering

Practical Application: This study demonstrates that a surface-enhanced Raman scattering (SERS)-based lateral flow strip (LFS) could be used as a rapid and sensitive method for *Escherichia coli* O157:H7 detection. Furthermore, this SERS-based LFS could achieve quantitative detection of the target, eliminating the defect of the traditional colloidal gold LFS, which is not quantifiable.

Introduction

Enterohemorrhagic *Escherichia coli* O157:H7 is a dangerous foodborne pathogen that can cause severe serious diseases with a low infectious dose (10 CFU) (Song et al., 2016). *E. coli* O157:H7 can contaminate water and food (Huang, Zhao, & Dou, 2018) and cause hemolytic uremic syndrome, bloody diarrhea, and even death (Pang et al., 2017). The World Health Organization has emphasized the significance of control and prevention of the spread of *E. coli* O157:H7 associated with food consumption (Luo et al., 2017). Therefore, sensitive and rapid detection of *E. coli* O157:H7 is crucial to ensure the health of consumers.

Current *E. coli* O157:H7 detection methods rely mostly on traditional microbial measuring methods and polymerase chain reaction (PCR) (Pang et al., 2017), which are standard approaches for *E. coli* O157:H7 detection. However, these methods are laborious, time consuming, and unsuitable for real-time screening (Abubakar et al., 2007). To date, several techniques have been established to replace traditional methods for *E. coli* O157:H7 detection, such as enzyme-linked immunosorbent assays (Bai, Huang, & Yang, 2007), electrochemical biosensors (Yan et al., 2017), and surface plasmon resonance immunosensors (Y. Wang, Ye, Si, & Ying, 2013). Although these methods possess high sensitivity, speed, and accuracy, they require expensive instruments and professional technicians. We concluded that these techniques are not suitable for real-time screening or point-of-care (POC) applications.

Lateral flow strips (LFSs) have received increasing attention in POC testing owing to their simplicity, speed, low cost, and robustness (He et al., 2010; P. Wang, Wang, Zhang, Su, & Luo, 2016). Gold nanoparticles (AuNPs) are widely used as labels in LFSs due to their unique optical properties and chemical stability (D. Zhang et al., 2018). However, AuNP-based LFSs have the drawbacks of low sensitivity and limited utility for quantitative analysis (Fu et al., 2016) and can be used only to detect analytes with relatively high concentrations. Recently, fluorescence, Raman, electrochemical, and magnetic labels were developed instead of AuNPs to achieve the quantitative and sensitive detection of

JFDS-2019-0516 Submitted 4/8/2019, Accepted 7/15/2019. *Authors Liu, Chen, Zhang, Du, Li, and Wang are with State Key Laboratory of Food Nutrition and Safety, Tianjin Univ. of Science and Technology, Tianjin 300457, China. Author Liu is with School of Life Sciences, North China Univ. of Science and Technology, Tangshan 063000, China. Author Wang is with Beijing Advanced Innovation Center for Food Nutrition and Human Health, Beijing Technology and Business Univ. (BTBU), Beijing 100048, China. Direct inquiries to author Wang (E-mail: s.wang@tust.edu.cn)*

doi: 10.1111/1750-3841.14766

Journal of Food Science A Publication of the Institute of Food Technologists

target analytes (Hwang, Lee, & Choo, 2016; Taranova, Berlina, Zherdev, & Dzantiev, 2015). However, fluorescence and magnetic labels suffer from chemical instability and high background signal, and fluorescence labels are subject to quenching. In contrast, surface-enhanced Raman scattering (SERS) nanotags are good candidates for LFS labels that can enhance the signal of Raman reporters by absorbing onto the nanoparticle surface, which is well known as a "hot spot" (Fu et al., 2016). Compared with fluorescence-based LFSs, the SERS-based LFS (SERS-LFS) has enhanced sensitivity and stability because the SERS signals originate from the rotation and vibration of Raman dyes (D. Zhang et al., 2018). Single nanotags could be detected due to the rational design of nanotags (Lim et al., 2011) and the ultrasensitivity and low interference of SERS detection (Liang et al., 2014).

The primary principles of the established SERS-LFS biosensors are consistent with those of the conventional LFSs based on AuNPs, except for the use of SERS nanotags. The SERS activity of AuNPs is weak and inapplicable for use as quantitative SERS nanotags in LFSs. In contrast, silver nanoparticles possess higher Raman scattering activity, but they suffer from poor chemical stability and biocompatibility (Becker et al., 2008). Au^{MBA}@Ag is a much brighter SERS tag than gold or silver nanoparticles because its surface is coated with Raman tags. The nanosized gap between Au and Ag has a strong electromagnetic field enhancement, which further improves the SERS signal intensity of the Raman dyes (Ngo, Gandra, Fales, Taylor, & Vo-Dinh, 2016). In addition, this sandwiched structure prevents the Raman dyes from leaking out and enhances their signal intensity. Furthermore, Au@Ag nanotags have not been previously used as optical and SERS dual probes in the detection of *E. coli* O157:H7.

In this study, we propose a SERS-LFS biosensor for the sensitive and quantitative detection of *E. coli* O157:H7. Au-Ag core-shell bimetallic nanotags with Raman dyes (4-methylthiobenzoic acid (MBA)) absorbed on the interior gap between the two metals (Au^{MBA}@Ag) were used as nanotags. The experimental conditions, including the Ag shell thickness, the running buffer, the pore diameter of the nitrocellulose (NC) membrane, and the amount of antibody conjugated to Au^{MBA}@Ag, were optimized to enhance the assay sensitivity. To our knowledge, this study is the first to use SERS-LFSs for the quantitative analysis of *E. coli* O157:H7 in a food matrix.

Materials and Methods

Materials and bacterial strains

Tetrachloroaurate (III) trihydrate ($HAuCl_4 \cdot 3H_2O$), trisodium citrate, 4-methylthiobenzoic (4-MBA), silver nitrate ($AgNO_3$), bovine serum albumin (BSA), and L-ascorbic acid were purchased from Sigma-Aldrich (St. Louis, MO). The NC membrane was obtained from Millipore (Bedford, MA, USA). Backing pads, sample pads, conjugate pads, and absorption pads were obtained from Shanghai Goldbio Tech Co., Ltd (China). The rabbit anti-*E. coli* O157:H7 polyclonal antibody was prepared in our laboratory, and the antirabbit IgG antibody produced in goat was purchased from Abcam (Abcam Beijing Zhongyuan, Ltd., Beijing, China). All other chemicals were of analytical reagent grade and used without further purification. Ultrapure water was purified with a Milli-Q water purification system (Madrid, Spain).

The standard strains used for testing the specificity and sensitivity of the SERS-LFS are listed in Table 1. A loopful of the strains was inoculated in 9 mL of Luria-Bertani (LB) broth (Beijing Land Bridge Technology Co., Ltd., Beijing, China) and incubated at 37 °C while shaking at 200 rpm for 18 to 24 hr. The grown cells were washed three times by repeating the centrifugation (10,000 × g, 30 s) and suspending the cells in buffer solution. The number of bacterial cells was counted by the plate counting method using plate counting agar (Beijing Land Bridge Technology Co., Ltd., Beijing, China).

Table 1–Bacterial strains used in this study.

Species	Source
Escherichia coli O157:H7	ATCC35150
Escherichia coli	CICC10305
Listeria monocytogenes	ATCC19115
Listeria monocytogenes	ATCC7644
Vibrio parahaemolyticus	ATCC17802
Salmonella enteritidis	CMCC50041
Salmonella enterica subsp. *enterica*	CICC10982
Salmonella enteritidis	ATCC13076
Salmonella Paratyphi-A	CICC21501
Salmonella Choleraesuis var. *Kunzendorf*	CICC21494
Shigella flexneri	CICC10865
Staphylococcus aureus	ATCC25923
Shigella sonnei	CICC21535
Enterobacter aerogenes	CICC10293
Campylobacter jejuni subsp. *jejuni*	ATCC33560
Staphylococcus epidermidis	CICC10294

CICC, China Center of Industrial Culture Collection; ATCC, American Type Culture Collection; CMCC, China Microbiological Culture Collection.

Instruments

The prepared Au^{MBA}@Ag was characterized by a Shimadzu UV-2300 UV–Vis spectrophotometer (Shimadzu, Japan) and JEM-2010 FEF transmission electron microscope (TEM, JEOL Ltd., Japan). The Raman spectra for the SERS nanotags were recorded with a confocal micro-Raman spectroscopic system (Renishaw, Gloucestershire, UK). The baseline of the obtained Raman spectra was corrected to zero with Renishaw Wire 4.2 software. Furthermore, the spectra were normalized by subtraction of the original spectrum of the LFSs with Origin 8.5 (OriginLab Corporation, Northampton, MA). Dispenser 93 (HM3035) (Shanghai Kinbio Tech. Co., Ltd., China) was used to immobilize the antibody on the NC membrane to form the control and test lines. The 3.7-mm-wide strips were prepared using a programmable cutter (Zeta Corporation, Gunpo, South Korea).

Synthesis of Au^{MBA} @ Ag SERS nanotags

The AuNPs and Au^{MBA}@Ag SERS nanotags were synthesized as described in our previous paper (H. B. Liu, Du, Zang, Li, & Wang, 2017), and the preparation procedure is presented in Figure 1A. The colloidal gold was first synthesized via the well-established citrate-reduction method (Frens, 1973) and was used as the template for the synthesis of Au^{MBA}@Ag nanotags. Here, 1 mol/L MBA (2.5 μL) was added to the AuNP solution (2 mL) and vigorously stirred for 5 min. MBA was conjugated to the surface of the AuNPs by the formation of Au−S bonds (B. Liu et al., 2012). Then, the Au^{MBA} was used as seeds to grow silver shells by the reduction of $AgNO_3$ with L-ascorbic acid. Briefly, 0.1 mol/L ascorbic acid (0.4 mL) was added to 2 mL of Au^{MBA} solution, and then 0.6, 1.2, and 2.4 mL of $AgNO_3$ solution (1 mM) were added dropwise to three separate tubes. Upon the addition of $AgNO_3$, the silver atoms were nucleated and eventually formed the silver shell around Au^{MBA}. The Ag shell thickness was optimized to achieve maximum Raman enhancement.

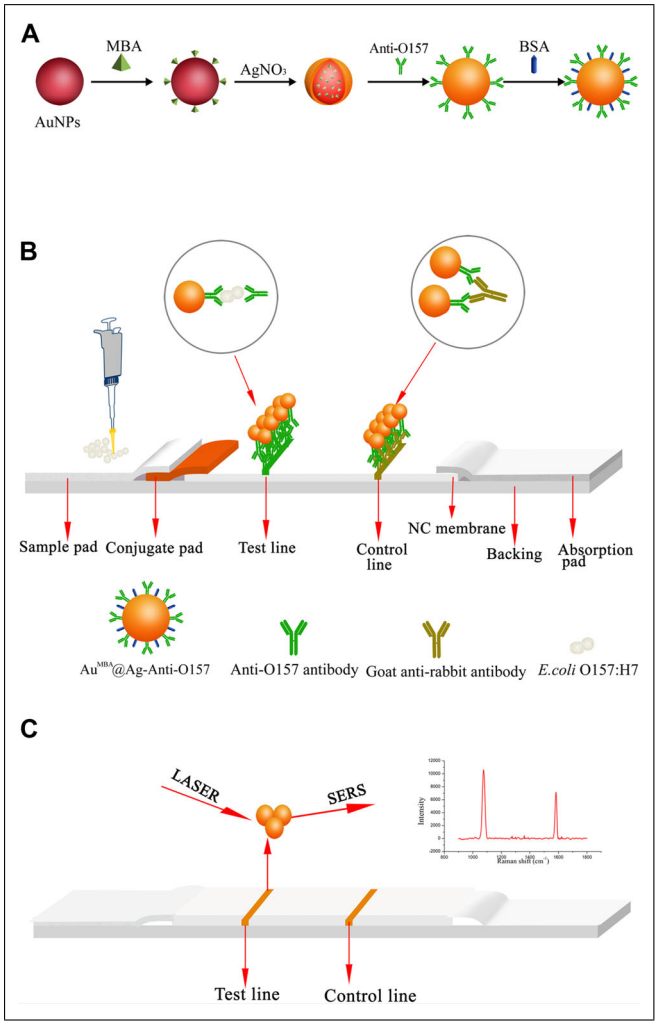

Figure 1–Schematic illustration of the preparation of Au^{MBA}@Ag-anti-*E. coli* O157:H7 antibody (A), the detection of *E. coli* O157:H7 with LFS (B), and the SERS detection of test line (C).

Conjugation of antibody with Au^{MBA}@Ag nanotags

Anti-*E. coli* O157:H7 pAb-labeled Au^{MBA}@Ag nanotags were prepared as follows: Different volumes of K_2CO_3 (1 mol/L) were added to the prepared Au^{MBA}@Ag (1 mL) to adjust the pH to 6.0, 6.5, 7.0, 7.5, 8.0, 8.5, 9.0, and 9.5. After 5 min, 200 μL of pH-adjusted Au^{MBA}@Ag solution was removed to 96-well plates, different amounts of antibody were added, and the solution was allowed to sit for 1 hr. UV–Vis was used to test the peak of the above solution at 360 nm. The optimum concentration of antibody and the optimum pH of Au^{MBA}@Ag nanotags were selected by observing the highest absorbance value at 360 nm and the brightest orange-yellow color. After optimization, defined volumes of the antibody and K_2CO_3 were added to 1 mL of Au^{MBA}@Ag solution and agitated for 1 hr at 4 °C. Subsequently, 20% BSA (20 μL) and 20% PEG20000 (10 μL) were added to the Au^{MBA}@Ag conjugates and allowed to react for another 30 min. The resulting solution was centrifuged, and the supernatant was discarded to remove the unbound antibody and chemicals. The residues containing SERS nanotags (Au^{MBA}@Ag-anti-*E. coli* O157:H7 pAb) were mixed with 200 μL of buffer containing 5% BSA, 0.025% Tween 20, and 1% sodium azide (pH = 7.4). The mixture was sprayed onto the conjugate pad at 25 μL/cm and then dried at room temperature for 8 hr.

Preparation of the SERS-LFs

Figure 1B and 1C illustrates the configuration and operating principle of the SERS-LFS for the analysis of *E. coli* O157:H7. The components of these SERS-LFSs include backing pads, absorbent pads, NC membranes, conjugate pads, and sample pads. To prepare the LF, the NC membrane was first affixed onto the backing pad. The goat antirabbit IgG and anti-*E. coli* O157:H7 pAb were sprayed on the NC membrane at a jetting rate of 0.9 μL/cm to produce the control and test line, respectively. The membrane was dried overnight at 37 °C. The absorbent pad and the conjugate pad were affixed onto either end of the NC membrane, and the sample pad was pasted to the end of the conjugate pad. All four components were assembled with 2 mm overlap, and the strips were cut into 3.7 mm in width. Finally, the LFSs were stored in a sealed bag with desiccative at room temperature for further use.

The measurement principle is based on sandwich-type reactions. When the *E. coli* O157:H7 solution was pipetted onto the sample pad, the liquid solution was moved toward the absorbent pad by capillary action. Then, *E. coli* O157:H7 reacted with the SERS immunoprobe, which was fixed onto the conjugate pad to form the target bacteria-pAb-Au^{MBA}@Ag complex. The immunocomplexes continued to flow to the test zone and were captured by the antibodies immobilized on the test line. The accumulation of the Au^{MBA}@Ag produced a characteristic orange-yellow band on the test line. Excessive SERS immunoprobe continued to migrate and was captured by the goat antirabbit IgG immobilized on the control line. Therefore, two orange-yellow bands appeared on the test line and the control line. The SERS signal intensity was proportional to the concentration of *E. coli* O157:H7. A Raman spectrometer was adopted to record the SERS signal intensity of MBA within Au^{MBA}@Ag, and a quantitative result was achieved. The presence of *E. coli* O157:H7 was verified through both the color change of the test line and the obtained SERS signal intensity of MBA. In the absence of *E. coli* O157:H7, only one orange-yellow band appeared on the control line, indicating that the test strip was working properly.

Selection of the NC membrane type and the optimum running buffer

The presence of surfactant in the running buffer and the pore size of the NC membrane are important factors regulating the binding time between antigen and antibody and affecting the sensitivity of the SERS-LFS. NC membranes HF180, HF135, and HF90 were tested to select which presented the brightest band. The flow rates of HF180, HF135, and HF90 are 180, 135, and 90 s/4 cm, respectively. Five types of running buffer (RB), RB1 (PBS + 0.1% Tween 20, pH = 8.0), RB2 (PBS + 0.1% Tween 20, pH 7.4), RB3 (0.01 mol/L PB buffer, pH = 7.4), RB4 (0.01 mol/L PBS buffer, pH = 5.7), and RB5 (0.01 mol/L PBS buffer, pH = 8.5) were tested. The running buffer that gave the brightest color on the test line and the lowest background color on the NC membrane was selected as the optimum running buffer in our experiment.

Sensitivity and specificity of the SERS-LFs

E. coli O157:H7 was cultured in LB broth at 37 °C for 18 to 24 hr. Total viable counts were determined by the plate counting method, which showed viable counts of *E. coli* O157:H7 at 5×10^8 CFU/mL. Simultaneously, bacterial suspension was heat killed at 100 °C for 10 min to ensure the safety of the experimenters (Gehring et al., 2004; Ruan, Yang, & Li, 2002) and 10-fold serially diluted with RB for further use. To test the

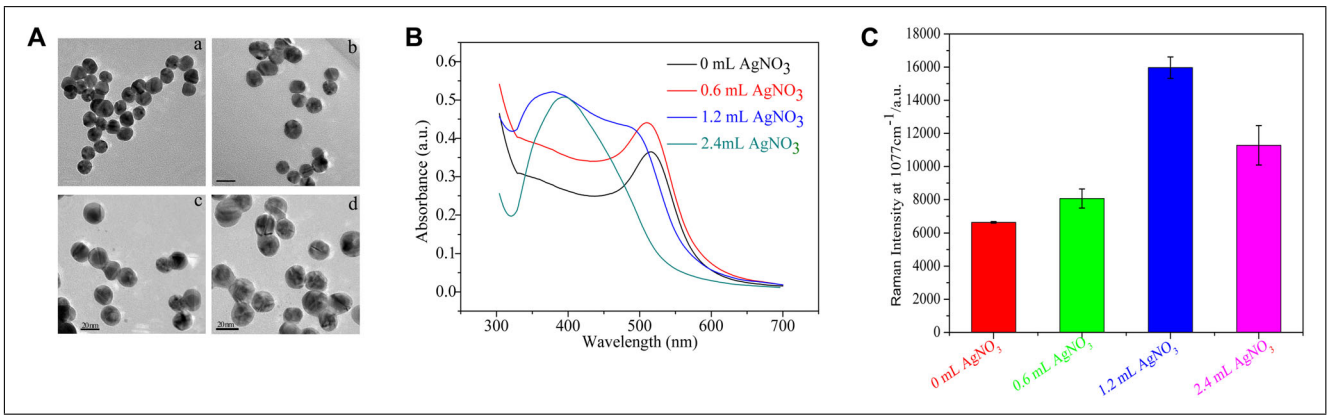

Figure 2–UV–Vis (A), TEM (B), and Raman signal intensity (C) of Au^{MBA}@Ag with different amounts of $AgNO_3$.

sensitivity of the SERS-LFs, 100 µL of *E. coli* O157:H7 solution at different concentrations was added onto the sample pad. The detection results were observed both by the naked eyes and by a Raman spectrometer (laser power, 25 mW, and integration time, 10 s). The signal intensities of MBA, which has characteristic Raman peaks at 1583 and 1077 cm^{-1}, were also obtained for the quantitative detection of *E. coli* O157:H7.

The specificity of the SERS-LFS was evaluated using *E. coli* O157:H7, *E. coli*, and 14 non-*E. coli* strains including *Listeria monocytogenes* (ATCC7644), *L. monocytogenes* (ATCC19115), *Vibrio parahaemolyticus*, *Salmonella enteritidis* (CMCC50041), *S. enteritidis* (ATCC13076), *Salmonella enterica* subsp. *enterica* (CICC10982), *Salmonella Choleraesuis* var. *Kunzendorf*, *Salmonella paratyphi-A*, *Shigella flexneri*, *S. sonnei*, *Staphylococcus aureus*, *S. epidermidis*, *Campylobacter jejuni* subsp. *jejuni*, and *Enterobacter aerogenes* (Table 1). Each strain was diluted to a concentration of 10^8 CFU/mL and tested by SERS-LFS. The running buffer alone was used as a negative control. All the experiments were repeated three times.

Application of SERS-LFS to food samples

To illustrate the feasibility and quantitative ability of the SERS-LFs, contaminated food samples were detected by this biosensor. Beef, chicken breast and milk were obtained from a local grocery store in Tianjin city, and the absence of *E. coli* O157:H7 was verified according to the National Standard method GB/4789.36-2016. These food matrices were selected as exemplars of solid and liquid matrices. *E. coli* O157:H7 was cultured in LB broth at 37 °C for 18 to 24 hr, and the culture was diluted to prepare different concentrations of *E. coli* O157:H7. The diluted bacteria were inoculated into selected food samples to achieve concentrations of 10^7, 10^6, 10^5, and 10^4 CFU/mL (CFU/g). Inoculated samples (25 g or 25 mL) were added to the running buffer at a ratio of 1:10 and thoroughly mixed. Aliquots of 1 mL from each food sample were collected and immediately heat killed at 100 °C for 10 min, and then 100 µL of the supernatant was pipetted onto the SERS-LFs. The detection results were determined by both the naked eyes and the Raman spectrum.

Results

Characterization and Raman signal intensity measurement of Au^{MBA}@Ag

First, the AuNPs were prepared, and TEM imaging (Figure 2Aa) demonstrated that the AuNPs were spherical in shape with an average diameter of 15.1 nm. The UV–Vis spectra (Figure 2B) of the AuNPs showed a strong and intense surface plasmon resonance absorption at 514 nm, indicating the monodispersity and uniform shape of the AuNPs. In the preparation of Au^{MBA}@Ag SERS nanotags, the thickness of the Ag shell heavily affected the Raman enhancement. Therefore, the amount of $AgNO_3$ was optimized. With the addition of $AgNO_3$, Ag continuously grew on the surface of Au^{MBA}. As shown in Figure 2Ab, Ac, and Ad, the edge of Au^{MBA}@Ag was much brighter than the center. In addition, with increasing silver shell thickness, the LSPR of Au^{MBA}@Ag exhibited a blueshift, indicating the formation of Au-Ag shell-gold nanoparticles. However, when the volume of $AgNO_3$ increased to 2.4 mL, the nanoparticles lost monodispersity (Figure 2Ad). Figure 2C displays the SERS signal intensity of Au^{MBA}@Ag with different silver shell thicknesses at 1077 cm^{-1}. It is clear that the Au^{MBA}@Ag exhibit higher SERS signal intensity than pure Au^{MBA}, and Au^{MBA}@Ag with 1.2 mL of $AgNO_3$ has the highest Raman intensity. Therefore, 1.2 mL of $AgNO_3$ was chosen as the optimum volume for use in preparing the SERS nanotags.

Optimization of the pH of Au^{MBA}@Ag and the addition of antibody

The pH of the Au^{MBA}@Ag solution and the concentration of antibody strongly affect the synthesis of the Au^{MBA}@Ag-anti-*E. coli* O157:H7 pAb. The coating efficiency of the antibody on Au^{MBA}@Ag will influence the sensitivity of the SERS-LFS. As shown in Table 2, the maximum UV–Vis absorbance peak is obtained at pH 8.5 with the addition of 4 µL of antibody. Therefore, the optimum pH for the conjunction of antibody with Au^{MBA}@Ag is 8.5, and the most suitable amount of antibody for

Table 2–Optimization of the conditions for the combination of Au^{MBA}@Ag nanoparticles and antibodies.

	Amount of antibody (µL)				
pH	2	3	4	5	6
6.5	0.303	0.433	0.498	0.596	0.576
7.0	0.322	0.435	0.527	0.573	0.582
7.5	0.339	0.447	0.552	0.579	0.593
8.0	0.343	0.485	0.588	0.595	0.513
8.5	0.359	0.493	0.605	0.510	0.522
9.0	0.357	0.443	0.585	0.492	0.513
9.5	0.344	0.424	0.569	0.498	0.506

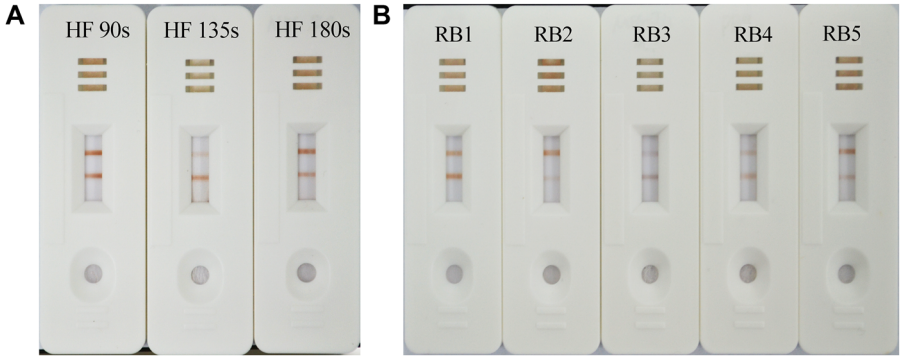

Figure 3–Optimization results of different types of NC membrane (A) and running buffer (B).

Figure 4–Digital photographs of the lateral flow strips at different concentrations of *E. coli* O157:H7 (5 × 10^8 to 5 × 10^4 CFU/mL).

200 μL of Au^{MBA}@Ag is 4 μL (1 mL of Au^{MBA}@Ag corresponds to an optimum antibody volume of 20 μL).

Optimize the NC membrane pore size and the running buffer

The type of NC membrane and running buffer had an important effect on this assay. NC membranes with different pore sizes were tested. As shown in Figure 3A, the band for HF90 was significantly brighter than the bands for HF135 and HF180. Therefore, HF90 is suitable for the migration of the *E. coli* O157:H7-antibody-Au^{MBA}@Ag sandwich complex and was selected for our subsequent experiments.

The running buffer solution also heavily influenced the flow rate of the immunocomplex. In addition, the selection of a suitable running buffer solution could increase the binding efficiency to target bacteria and capture antibodies. In Figure 3B, the orange-yellow band for RB1 was significantly stronger than that of the other four buffer solutions. Based on this result, RB1 was used in the subsequent experiment.

Sensitivity and quantitative ability of SERS-LFs

Optimum conditions for the use of the SERS-LFS for *E. coli* O157:H7 detection were established. *E. coli* O157:H7 solutions in the range of 5 × 10^8 to 5 × 10^3 CFU/mL were prepared by diluting *E. coli* O157:H7 with RB1. As shown in Figure 4, as the *E. coli* O157:H7 concentration increased, the orange-yellow color of the test line was proportionally increased. When the concentration of *E. coli* O157:H7 was below 5 × 10^5 CFU/mL, the color of the test line was not visible. Therefore, the visual LOD of the SERS-LFs was 5 × 10^5 CFU/mL.

Quantitative analysis of *E. coli* O157:H7 was obtained by measuring the SERS signal intensity of the test line. As shown in Figure 5A, the Raman intensities increased concomitantly with increasing *E. coli* O157:H7 concentration. Based on this result, calibration curves were obtained in the form of *E. coli* O157:H7 concentration versus SERS peak intensities centered at 1077 cm^{-1}, which is higher than that at 1583 cm^{-1} (Figure 5B). The linear curve has good linearity between the Raman signal intensity and the logarithm of *E. coli* O157:H7 concentration (R^2 = 0.9947).

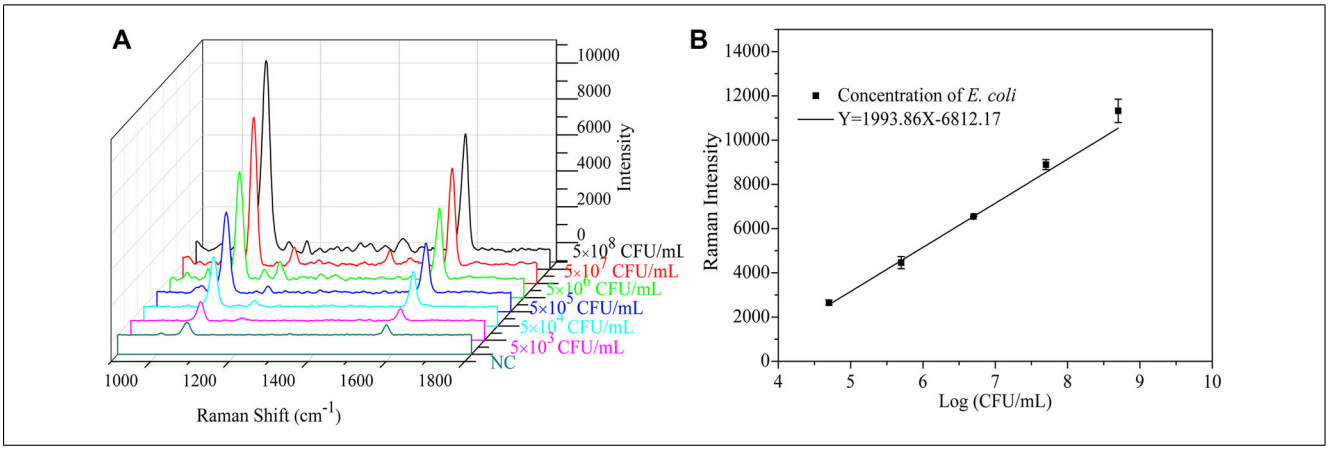

Figure 5–(A) SERS spectral intensity of Au^{MBA}@Ag on test lines from different concentrations of *E. coli* O157:H7. (B) Calibration curve for *E. coli* O157:H7 detection of variations in MBA SERS signal intensity centered at 1077 cm^{-1}.

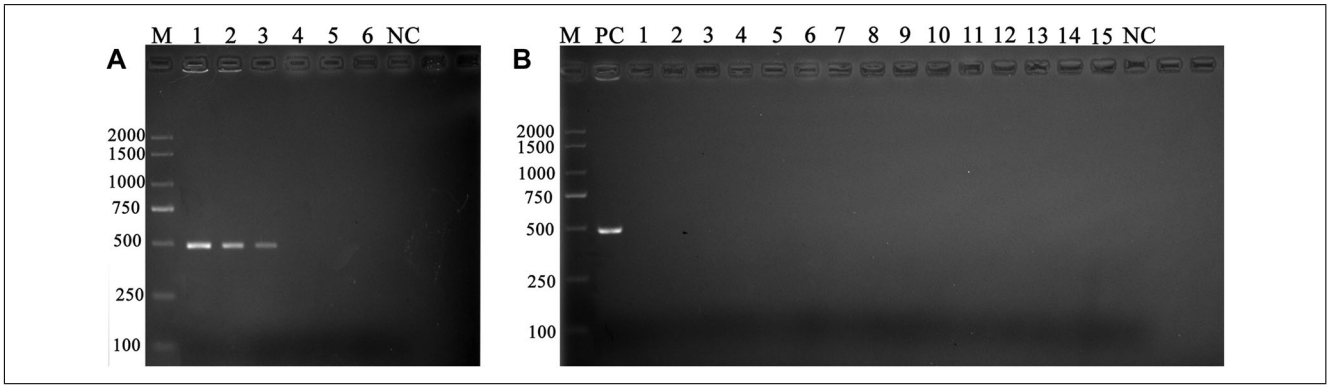

Figure 6–(A) Agarose gel image of PCR for the detection of *E. coli* O157:H7. (B) Molecular specificity of the PCR-AGE using *E. coli* O157:H7 and 15 other bacteria.

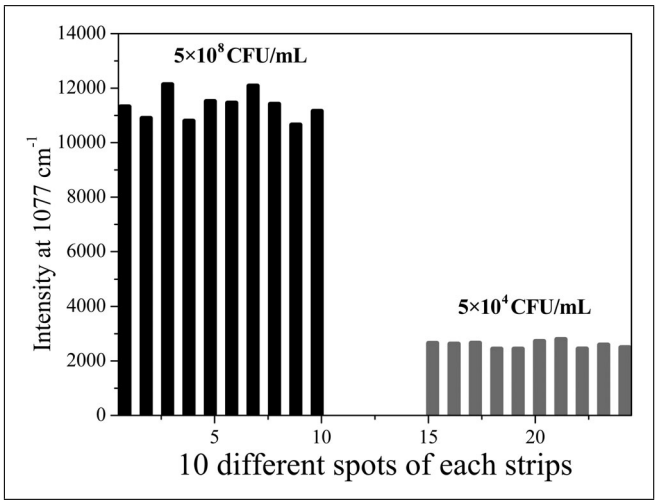

Figure 7–SERS intensities of MBA at 1077 cm^{-1} from 10 different spots on the middle parts of the test lines on the strips with *E. coli* O157:H7 concentrations of 5 × 10^8 and 5 × 10^4 CFU/mL.

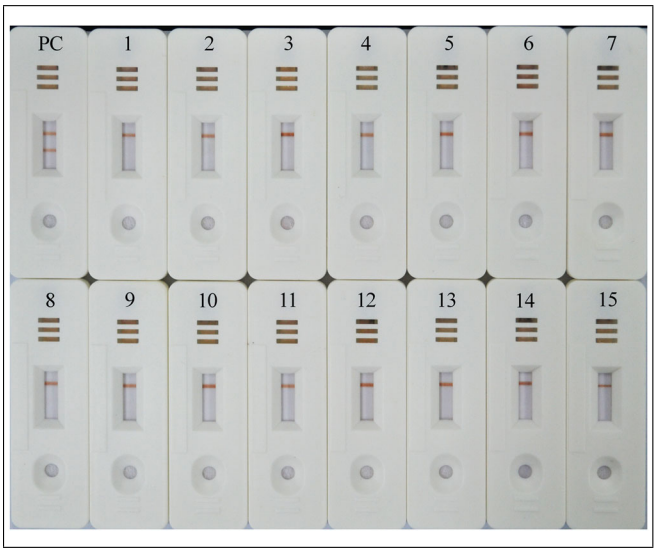

Figure 8–Detection specificity of the SERS-based lateral flow strip assay. PC positive control (*E. coli* O157:H7), 1 *E. coli*, 2 *L. monocytogenes* (ATCC19115), 3 *L. monocytogenes* (ATCC7644), 4 *V. parahaemolyticus*, 5 *S. enteritidis* (CMCC50041), 6 *S. enterica* subsp. *enterica* (CICC10982), 7 *S. enteritidis* (ATCC13076), 8 *S. paratyphi-A*, 9 *S. Choleraesuis* var. *Kunzendorf*, 10 *S. flexneri*, 11 *S. aureus*, 12 *S. sonnei*, 13 *E. aerogenes*, 14 *C. jejuni* subsp. *jejuni*, 15 *S. epidermidis*.

Error bars represent the standard deviations of five detections. When the *E. coli* O157:H7 concentration was 5 × 10^3 CFU/mL, the Raman intensity of MBA at 1077 cm^{-1} was 1036.21, which was only 1.49-fold higher than the Raman intensity of 696.99 in the negative control. Thus, the SERS-LFS detection limit was 5 × 10^4 CFU/mL with a Raman intensity of 2769.59, which was 3.9-fold higher than the Raman intensity of the negative control (S/N > 3).

PCR combined with agarose gel electrophoresis (AGE) was also applied to pure *E. coli* O157:H7 cultures with different concentrations ranging from 5 × 10^8 to 5 × 10^3 CFU/mL. As shown in Figure 6A, the detection limit of PCR-AGE was only 5 × 10^6 CFU/mL. Furthermore, only *E. coli* O157:H7 produced a visible band at 499 bp (Figure 6B).

Reproducibility of the SERS-LFS

To investigate the reproducibility of the SERS signals, the signals of ten different points on the middle of the test lines from two strips were tested. *E. coli* O157:H7 concentrations of 5 × 10^8 and 5 × 10^4 CFU/mL were applied to the two test strips. As shown in Figure 7, the RSD values of 10 different spots on each test line were 4.39% and 4.89%, indicating high precision of the SERS signal.

Specificity of the SERS-LFs

The specificity of the developed method depends on the specific affinity of the antibody to the target bacteria. The specificity of this SERS-LFS was evaluated by testing against *E. coli* O157:H7, *E. coli* and other microorganisms, including *L. monocytogenes* (ATCC19115), *L. monocytogenes* (ATCC7644), *V. parahaemolyticus*, *S. enteritidis* (CMCC50041), *S. enterica* subsp. *enterica* (CICC10982), *S. enteritidis* (ATCC13076), *S. paratyphi-A*, *S. Choleraesuis* var. *Kunzendorf*, *S. flexneri*, *S. aureus*, *S. sonnei*, *E. aerogenes*, *C. jejuni* subsp. *jejuni*, and *S. epidermidis*. As illustrated in Figure 8, only *E. coli* O157:H7 produced a positive reaction, while *E. coli* and other microorganisms had colorless T-lines. This result confirms that the SERS-LFS possesses high specificity and selectivity for the analysis of *E. coli* O157:H7. Furthermore, the SERS-LFS results are consistent with the PCR-AGE results.

Application of SERS-LFs in food samples

To evaluate the anti-interference ability of the developed method in food samples, simulated chicken breast, beef, and milk

Table 3–Detection results and recoveries of *E. coli* O157:H7 in milk, chicken breast, and beef using the SERS-based lateral flow strips.

Sample	Spiked concentration (CFU/mL)	Results based on naked eye assessment	Results based on SERS	Recoveries (%)
Milk 1	5×10^7	+,+,+	+,+,+	104.54 ± 1.46
Milk 2	5×10^6	+,+,+	+,+,+	98.78 ± 2.25
Milk 3	5×10^5	+,+,+	+,+,+	96.09 ± 2.07
Milk 4	5×10^4	−,−,−	+,+,+	97.50 ± 2.92
Chicken breast 1	5×10^7	+,+,+	+,+,+	98.74 ± 0.98
Chicken breast 2	5×10^6	+,+,+	+,+,+	107.59 ± 2.09
Chicken breast 3	5×10^5	+,+,+	+,+,+	105.04 ± 3.99
Chicken breast 4	5×10^4	−,−,−	+,+,+	94.19 ± 3.14
Beef 1	5×10^7	+,+,+	+,+,+	103.22 ± 1.99
Beef 2	5×10^6	+,+,+	+,+,+	98.92 ± 1.95
Beef 3	5×10^5	+,+,+	+,+,+	95.52 ± 2.79
Beef 4	5×10^4	−,−,−	+,+,+	96.93 ± 0.89

Visual and SERS-based assessment of the test line: (+) positive result, (−) negative result.

samples spiked with *E. coli* O157:H7 were tested using SERS-LFs. The *E. coli* O157:H7 in the spiked samples was evaluated under the same conditions described above. The total recovered colonies were calculated from the obtained Raman intensities and the calibration curve (Roy et al. 2018; Zeinhom et al., 2018). As shown in Table 3, the recoveries of *E. coli* O157:H7 in food samples were 95.52% to 107.59%. The detection limit of *E. coli* O157:H7 in milk, chicken breast, and beef was 5×10^4 CFU/mL. Therefore, the application performance clearly illustrated that the SERS-LFS based on Au^{MBA}@Ag labeling and SERS detection can efficiently and quantitatively detect *E. coli* O157:H7 in food samples.

Discussion

Au^{MBA}@Ag was used as labels in the SERS-LFS to achieve quantitative detection. In addition, the SERS enhancement of Au^{MBA}@Ag will affect the sensitivity of the LFS (M. Li et al., 2014). The SERS signal intensity of MBA is enhanced by the electromagnetic field between the gold core and silver shell, and the thickness of the silver shell was optimized to achieve Raman signals with ultrahigh intensity and reproducibility. As shown in Figure 2Aa, Ab, Ac, and Ad, the thickness of the Ag shells increased with increasing amounts of $AgNO_3$ in the range of 0, 0.6, 1.2, and 2.4 to 2 mL of Au^{MBA} solution. Figure 2B illustrates that the LSPR of Au^{MBA}@Ag exhibits a blueshift with increasing silver shell thickness. This result agrees with the traditional Mie scattering theory (Lee et al., 2007; Moskovits, Srnovasloufova, & Vlckova, 2002) and indicates the formation of silver-gold core-shell nanoparticles. The SERS intensity of Au^{MBA}@Ag at 1077 cm^{-1} is closely related to the thickness of the Ag shell (Figure 2C). When up to 1.2 mL of $AgNO_3$ was added, the enhancement of the Raman signal increased with the amount of $AgNO_3$. Further increases in $AgNO_3$ decreased the Raman enhancement. This phenomenon can be interpreted as a larger silver shell thickness damping the laser excitation of MBA and hindering the output of MBA's Raman signal (Zhao et al., 2015). Furthermore, a larger shell thickness will affect the coupling between the gold core and silver shell, and reduce the electromagnetic enhancement effect (D. Zhang et al., 2018). As shown in Figure 2Ad, the monodispersity of Au^{MBA}@Ag was destroyed, and the steric effect hindered efficient diffusion in the NC membrane. Therefore, it was necessary to optimize the thickness of the Ag shell of Au^{MBA}@Ag nanoparticles, and our results showed that 1.2 mL of $AgNO_3$ to 2 mL of colloidal gold was the optimal ratio to achieve the strongest Raman enhancement.

To maximize the analytical sensitivity, the pH of Au^{MBA}@Ag, the addition of antibody, the type of NC membrane, the running buffer, and the integration time of the laser were optimized. First, the antibody amount and the pH of the Au^{MBA}@Ag solution for labeling were optimized to enhance the stability of the nanoparticles. The antibody will efficiently absorb on the surface of Au^{MBA}@Ag only when the pH is maintained near the isoelectric point (Song et al., 2016). As shown in Table 2, the optimum condition for antibody and Au^{MBA}@Ag connection was obtained at pH 8.5 with the addition of 4 μL of antibody. At this condition, the maximum UV–Vis absorbance value was achieved, while the addition of antibody was relatively low. Second, the type of NC membrane and running buffer affect the flow velocity of samples and then influence the assay sensitivity (Gao et al., 2017). Generally, the presence of surfactant and the pore size of the NC membrane affect the flow rate of samples on the NC membrane and further regulate the binding time of antibody and target bacteria. Figure 3A reveals that HF90 provides a suitable capillary flow rate and gives a satisfactory orange-yellow band. HF135 and HF180, which have smaller pore sizes, were not suitable for this assay. Therefore, a larger pore size of the NC membrane will facilitate the movement of bacteria with larger diameters. In addition, RB1 was the optimal running buffer (Figure 3B). The presence of Tween 20 facilitated better flow of immuno-nanoparticles through the NC membrane and mitigated the nonspecific absorption of immuno-nanoparticles on the test line. This result is in agreement with the literature (J. Liu, Mazumdar, & Lu, 2006; Rivas et al., 2015) reporting that the presence of surfactant in running buffer can significantly reduce the background signal because of nonspecific binding on the membrane. Therefore, HF90 and RB1 were selected as the optimum combination. During the experiment process, different concentrations of *E. coli* O157:H7 will be added

Table 4–Comparison of the detection limits of different lateral flow strip assays.

Method	Target	Detection time	Quantification	LOD	Reference
PCR-LFS	*S. aureus*	49 hr	No	2×10^0	Zhang et al., 2017
Superparamagnetic NP-LFS	*L. monocytogenes*	20 min	10^4 to 10^8	10^4	Shi et al., 2015
Conventional LFS	*Shigella boydii* *E. coli* O157:H7	5 to 10 min	No	10^6	Song et al., 2016
LFS-image analysis	*E. coli* O157:H7	20 min	No	10^4	Kim et al., 2013
Immunomagnetic separation-LFS	*E. coli* O157:H7	50 min	No	2.8×10^3	Huang et al., 2016
SERS-LFS	*E. coli* O157:H7	15 min	10^4 to 10^8	10^4	This study
PCR-AGE	*E. coli* O157:H7	1.5 hr	No	5×10^6	This study

to running buffer or food samples. The *E. coli* O157:H7 should be heat-killed to ensure the safety of the experimenters and prevent these bacteria from polluting the environment . And this step can be omitted during the actual application process. Finally, the laser power of the Raman spectrometer was tuned at 25 mW, and the integration time was set to 10 s. Based on our experiments, the use of higher laser powers and longer integration times generated enough heat to destroy the NC membrane.

While LFSs have been successfully used in the detection of numerous pathogens, such as *Pseudomonas aeruginosa* (Chen et al., 2016), *S. boydii*, *E. coli* O157:H7 (Song et al., 2016), and *Staphylococcus aureus* (H. Zhang et al., 2017), they possess major limitations including low sensitivity and the inability to achieve quantitative results. To resolve these drawbacks, SERS-LFSs were established in this experiment. SERS spectroscopy is a highly sensitive detection platform that allows trace and nondestructive detection (J. F. Li et al., 2010). The combination of SERS and LFSs is an ideal technique to lower the detection limit and permit quantitative detection. All the test procedures can be completed within 15 min. The analytical characteristics of these SERS-LFSs are compared with those of other techniques in Table 4. Compared with other methods, the quantitative SERS-LFS is sensitive, fast, low cost, and fit for POC detection. Furthermore, food sample analysis demonstrated that SERS-LFS can efficiently and rapidly detect bacteria.

Conclusion

We established an SERS-LFS for the quantitative and sensitive analysis of *E. coli* O157:H7. Antibody-modified Au^{MBA}@Ag nanotags were employed in the SERS-LFSs, and the specific SERS signal intensity of MBA was used for quantification. With carefully optimized experimental conditions, the limit of detection values of this assay for *E. coli* O157:H7 is estimated to be 5×10^4 CFU/mL, which is 10-fold higher sensitivity than that of colorimetric LFSs. SERS-LFSs have a dynamic range from 5×10^8 to 5×10^4 CFU/mL with a coefficient of determination of 0.9947. Testing with the SERS-LFSs was completed in 15 min and had the advantages of high specificity, small sample volume, and the elimination of sample pretreatment. Therefore, this SERS-LFS could be directly used to detect *E. coli* O157:H7 in food samples, representing an optimistic outlook for the future. Obviously, the combination of this SERS-LFS with a portable Raman spectrometer can increase its onsite applicability. This newly developed assay has great potential for the detection of additional and multiple foodborne pathogens and the detection limit of this SERS-LF could be lowered by using other nanoparticles to enhance Raman scattering. Thus, this SERS-LFS may provide a practical method to monitor multiple bacteria species in food samples.

Acknowledgments

This work was supported by The National Key Research and Development Program of China (No. 2017YFD0400704), a project of the Ministry of Science and Technology of the People's Republic of China (project No. 2014BAD04B03), The Excellent Doctoral Fund Project (No. 2016003), and Hebei Province Key Research and Development Plan Self-funded Projects (18227533).

Author Contributions

Haibin Liu participated in every stage of the study, including designing and performing the experiments and preparing the manuscript. Chunyang Chen and Chenning Zhang performed some experiments. Xinjun Du and Ping Li reviewed and edited the manuscript. Shuo Wang designed the research. All authors read and approved the manuscript.

References

Abubakar, I., Irvine, L., Aldus, C. M., Wyatt, G. M., Fordham, R., Schelenz, S., . . . Hunter, P. R. (2007). A systematic review of the clinical, public health and cost-effectiveness of rapid diagnostic tests for the detection and identification of bacterial intestinal pathogens in faeces and food. *Health Technology Assessment*, *11*(36), 1–216.

Bai, Y., Huang, W. C., & Yang, S. T. (2007). Enzyme-linked immunosorbent assay of *Escherichia coli* O157:H7 in surface enhanced poly(methyl methacrylate) microchannels. *Biotechnology and Bioengineering*, *98*(2), 328–339. https://doi.org/10.1002/bit.21429

Becker, J., Zins, I., Jakab, A., Khalavka, Y., Schubert, O., & Sönnichsen, C. (2008). Plasmonic focusing reduces ensemble linewidth of silver-coated gold nanorods. *Nano Letters*, *8*(6), 1719–1723. https://doi.org/10.1021/nl080720k

Chen, Y., Cheng, N., Xu, Y., Huang, K., Luo, Y., & Xu, W. (2016). Point-of-care and visual detection of *P. aeruginosa* and its toxin genes by multiple LAMP and lateral flow nucleic acid biosensor. *Biosensors & Bioelectronics*, *81*, 317–323. https://doi.org/10.1016/j.bios.2016.03.006

Frens, G. (1973). Controlled nucleation for the regulation of the particle size in monodisperse gold suspensions. *Nature Physical Science*, *241*, 20–22. https://doi.org/10.1038/physci241020a0

Fu, X., Cheng, Z., Yu, J., Choo, P., Chen, L., & Choo, J. (2016). A SERS-based lateral flow assay biosensor for highly sensitive detection of HIV-1 DNA. *Biosensors & Bioelectronics*, *78*, 530–537. https://doi.org/10.1016/j.bios.2015.11.099

Gao, X., Zheng, P., Kasani, S., Wu, S., Yang, F., Lewis, S., . . . Simpkins, J. W. (2017). Paper-based surface-enhanced Raman scattering lateral flow strip for detection of neuron-specific enolase in blood plasma. *Analytical Chemistry*, *89*(18), 10104–10110. https://doi.org/10.1021/acs.analchem.7b03015

Gehring, A. G., Irwin, P. L., Reed, S. A., Tu, S. I., Andreotti, P. E., Akhavan-Tafti, H., & Handley, R. S. (2004). Enzyme-linked immunomagnetic chemiluminescent detection of *Escherichia coli* O157: H7. *Journal of immunological methods*, *293*(1-2), 97–106. https://doi.org/10.1016/j.jim.2004.07.004

He, Y., Zeng, K., Gurung, A. S., Baloda, M., Xu, H., Zhang, X., & Liu, G. (2010). Visual detection of single-nucleotide polymorphism with hairpin oligonucleotide-functionalized gold nanoparticles. *Analytical Chemistry*, *82*(17), 7169–7171. https://doi.org/10.1021/ac101275s

Huang, Z., Cui, X., Xie, Q. Y., Liu, D. F., & Lai, W. H. (2016). A novel method using immunomagnetic separation with a fluorescent nanobeads lateral flow assay for the rapid detection of low-concentration Escherichia coli O157: H7 in raw milk. *Journal of dairy science*, *99*(12), 9581-9585. https://doi.org/10.3168/jds.2016-11780

Huang, H., Zhao, G., & Dou, W. (2018). Portable and quantitative point-of-care monitoring of *Escherichia coli* O157:H7 using a personal glucose meter based on immunochromatographic assay. *Biosensors & Bioelectronics*, *107*, 266–271. https://doi.org/10.1016/j.bios.2018.02.027

Hwang, J., Lee, S., & Choo, J. (2016). Application of a SERS-based lateral flow immunoassay strip for the rapid and sensitive detection of staphylococcal enterotoxin B. *Nanoscale*, *8*(22), 11418–11425. https://doi.org/10.1039/c5nr07243c

Kim, G., Moon, J. H., Park, S. B., Jang, Y. J., Lim, J., & Mo, C. (2013). Image analysis of a lateral flow strip sensor for the detection of Escherichia coli O157: H7. *Journal of Biosystems Engineering*, *38*(4), 335–340. https://doi.org/10.5307/JBE.2013.38.4.335

Lee, S., Kim, S., Choo, J., Shin, S. Y., Lee, Y. H., Choi, H. Y., . . . Oh, C. H. (2007). Biological imaging of HEK293 cells expressing PLCgamma1 using surface-enhanced Raman microscopy. *Analytical Chemistry*, *79*(3), 916–922. https://doi.org/10.1021/ac061246a

Li, J. F., Huang, Y. F., Ding, Y., Yang, Z. L., Li, S. B., Zhou, X. S., . . . Wu, D. Y. (2010). Shell-isolated nanoparticle-enhanced Raman spectroscopy. *Nature*, *464*(1), 392–395. https://doi.org/10.1038/nature08907

Li, M., Yang, H., Li, S., Zhao, K., Li, J., Jiang, D., . . . Deng, A. (2014). Ultrasensitive and quantitative detection of a new Î²-agonist phenylethanolamine A by a novel immunochromatographic assay based on surface-enhanced Raman scattering (SERS). *Journal of Agricultural and Food Chemistry*, *62*(45), 10896–10902. https://doi.org/10.1021/jf503599x

Liang, J., Liu, H., Lan, C., Fu, Q., Huang, C., Luo, Z., . . . Tang, Y. (2014). Silver nanoparticle enhanced Raman scattering-based lateral flow immunoassays for ultrasensitive detection of the heavy metal chromium. *Nanotechnology*, *25*(49), 495–501. https://doi.org/10.1088/0957-4484/25/49/495501

Lim, D. K., Jeon, K. S., Hwang, J. H., Kim, H., Kwon, S., Suh, Y. D., & Nam, J. M. (2011). Highly uniform and reproducible surface-enhanced Raman scattering from DNA-tailorable nanoparticles with 1-nm interior gap. *Nature Nanotechnology*, *6*(7), 452–460. https://doi.org/10.1038/nnano.2011.79

Liu, B., Han, G., Zhang, Z., Liu, R., Jiang, C., Wang, S., & Han, M. Y. (2012). Shell thickness-dependent Raman enhancement for rapid identification and detection of pesticide residues at fruit peels. *Analytical Chemistry*, *84*(1), 255–261. https://doi.org/10.1021/ac202452t

Liu, H. B., Du, X. J., Zang, Y. X., Li, P., & Wang, S. (2017). A SERS-based lateral flow strip biosensor for simultaneous detection of *Listeria monocytogenes* and *Salmonella enterica* serotype Enteritidis. *Journal of Agricultural and Food Chemistry*, *65*, 10290–10299. https://doi.org/10.1021/acs.jafc.7b03957

Liu, J., Mazumdar, D., & Lu, Y. (2006). A simple and sensitive "dipstick" test in serum based on lateral flow separation of aptamer-linked nanostructures. *Angewandte Chemie*, *45*(47), 7955–7959. https://doi.org/10.1002/ange.200603106

Luo, K., Hu, L., Guo, Q., Wu, C., Wu, S., Liu, D., . . . Lai, W. (2017). Comparison of 4 label-based immunochromatographic assays for the detection of *Escherichia coli* O157:H7 in milk. *Journal of Dairy Science*, *100*, 5176–5178. https://doi.org/10.3168/jds.2017-12554

Moskovits, M., Srnovasloufova, I., & Vlckova, B. (2002). Bimetallic Ag-Au nanoparticles: Extracting meaningful optical constants from the surface-plasmon extinction spectrum. *Journal of Chemical Physics*, *116*(23), 10435–10446. https://doi.org/10.1063/1.1449943

Ngo, H. T., Gandra, N., Fales, A. M., Taylor, S. M., & Vo-Dinh, T. (2016). Sensitive DNA detection and SNP discrimination using ultrabright sers nanorattles and magnetic beads for malaria diagnostics. *Biosensors & Bioelectronics*, *81*, 8–14. https://doi.org/10.1016/j.bios.2016.01.073

Pang, B., Zhao, C., Li, L., Song, X., Xu, K., Wang, J., . . . Song, D. (2017). Development of a low-cost paper-based ELISA method for rapid *Escherichia coli* O157:H7 detection. *Analytical Biochemistry*, *542*, 58–62. https://doi.org/10.1016/j.ab.2017.11.010

Rivas, L., de la Escosura-Muniz, A., Serrano, L., Altet, L., Francino, O., Sanchez, A., & Merkoci, A. (2015). Triple lines gold nanoparticle-based lateral flow assay for enhanced and

simultaneous detection of *Leishmania* DNA and endogenous control. *Nano Research*, *8*(11), 3704–3714. https://doi.org/10.1007/s12274-015-0870-3

Roy, E., Patra, S., Tiwari, A., Madhuri, R., & Sharma, P. K. (2018). Single cell imprinting on the surface of Ag-ZnO bimetallic nanoparticle modified graphene oxide sheets for targeted detection, removal and photothermal killing of *E. Coli*. *Biosensors & Bioelectronics*, *89*, 620–626. https://doi.org/10.1016/j.bios.2015.12.085

Ruan, C., Yang, L., & Li, Y. (2002). Immunobiosensor chips for detection of *Escherichia coli* O157: H7 using electrochemical impedance spectroscopy. *Analytical Chemistry*, *74*, 4814–4820. https://doi.org/10.1021/ac025647b

Shi, L., Wu, F., Wen, Y., Zhao, F., & Xiang, J. J. (2015). A novel method to detect Listeria monocytogenes via superparamagnetic lateral flow immunoassay. *Analytical and bioanalytical chemistry*, *407*, 529–535. https://doi.org/10.1007/s00216-014-8276-8

Song, C., Liu, C., Wu, S., Li, H., Guo, H., Yang, B., . . . Zeng, H. (2016). Development of a lateral flow colloidal gold immunoassay strip for the simultaneous detection of *Shigella boydii* and *Escherichia coli* O157:H7 in bread, milk and jelly samples. *Food Control*, *59*, 345–351. https://doi.org/10.1016/j.foodcont.2015.06.012

Taranova, N. A., Berlina, A. N., Zherdev, A. V., & Dzantiev, B. B. (2015). 'Traffic light' immunochromatographic test based on multicolor quantum dots for the simultaneous detection of several antibiotics in milk. *Biosensors & Bioelectronics*, *63*(2), 255–261. https://doi.org/10.1016/j.bios.2014.07.049

Wang, P., Wang, R., Zhang, W., Su, X., & Luo, H. (2016). Novel fabrication of immunochromatographic assay based on up conversion phosphors for sensitive detection of clenbuterol. *Biosensors & Bioelectronics*, 77(6-7), 866–870. https://doi.org/10.1016/j.bios.2015.10.053

Wang, Y., Ye, Z., Si, C., & Ying, Y. (2013). Monitoring of *Escherichia coli* O157:H7 in food samples using lectin based surface plasmon resonance biosensor. *Food Chemistry*, *136*(3–4), 1303–1308. https://doi.org/10.1016/j.foodchem.2012.09.069

Yan, L., Xiong, Y., Fang, L., Jiang, L., Hui, H., Deng, J., . . . Zheng, J. (2017). An electrochemical strategy using multifunctional nanoconjugates for efficient simultaneous detection of *Escherichia coli* O157: H7 and *Vibrio cholerae* O1. *Theranostics*, 7(4), 935–944. https://doi.org/10.7150/thno.17544

Zeinhom, M. M. A., Wang, Y., Song, Y., Zhu, M. J., Lin, Y., & Du, D. (2018). A portable smart-phone device for rapid and sensitive detection of *E. coli* O157: H7 in yoghurt and egg. *Biosensors & Bioelectronics*, *99*, 479–485. https://doi.org/10.1016/j.bios.2017.08.002

Zhang, D., Huang, L., Liu, B., Ni, H., Sun, L., Su, E., . . . Zhao, X. (2018). Quantitative and ultrasensitive detection of multiplex cardiac biomarkers in lateral flow assay with core-shell SERS nanotags. *Biosensors & Bioelectronics*, *106*, 204–211. https://doi.org/10.1016/j.bios.2018.01.062

Zhang, H., Ma, L., Ma, L., Hua, M. Z., Wang, S., & Lu, X. (2017). Rapid detection of methicillin-resistant *Staphylococcus aureus* in pork using a nucleic acid-based lateral flow immunoassay. *International Journal of Food Microbiology*, *243*, 64–69. https://doi.org/10.1016/j.ijfoodmicro.2016.12.003

Zhao, X., Xue, J., Mu, Z., Yin, H., Meng, L., & Gu, Z. (2015). Gold nanoparticle incorporated inverse opal photonic crystal capillaries for optofluidic surface enhanced Raman spectroscopy. *Biosensors & Bioelectronics*, *72*, 268–274. https://doi.org/10.1016/j.bios.2015.05.036